

Intense Picosecond X-Ray Pulses from Laser Plasmas by Use of Nanostructured “Velvet” Targets

G. Kulcsár,¹ D. AlMawlawi,³ F. W. Budnik,¹ P. R. Herman,² M. Moskovits,³ L. Zhao,¹ and R. S. Marjoribanks¹

¹*Department of Physics, University of Toronto, Toronto, Canada M5S 1A7
and Photonics Research Ontario, Toronto, Ontario, Canada M5S 1A7*

²*Department of Electrical and Computer Engineering, University of Toronto, Toronto, Canada M5S 3G4*

³*Department of Chemistry, University of Toronto, Toronto, Canada M5S 3H6*

(Received 28 December 1998)

We describe the optical, radiative, and laser-plasma physics of a new type of nanostructured surface especially promising as a very high absorption target for high-peak-power subpicosecond laser-matter interaction. This oriented-nanowire material, irradiated by 1 ps pulses at intensities up to 10^{17} W cm⁻², produces picosecond soft x-ray pulses 50× more efficiently than do solid targets. We compare this to “smoke” or metallic clusters, and solid nanogroove-grating surfaces; the “metal-velvet” targets combine the high yield of smoke targets with the brief emission of grating surfaces.

PACS numbers: 52.40.Nk, 52.25.Nr, 52.50.Jm

The introduction of ultraintense picosecond and subpicosecond chirped-pulse amplification lasers has brought a flurry of research interest in developing and using high peak-brightness soft-x-ray and x-ray sources. High-harmonic generation from laser interaction with noble gases has recently produced presumably coherent soft x rays in the “water window” between absorption edges of carbon and oxygen [1], and analogous generation from near-solid-density laser-produced plasmas has promise of much more efficient conversion [2]. Such sources show little immediate prospect of extension to high-peak-flux sources of kiloelectron-volt photons, needed, for example, in single-event pulse-probe studies in materials science [3]. Certain tabletop extreme ultraviolet (XUV) and soft-x-ray laser schemes require intense picosecond pulses of keV x-rays as pump sources [4]. Studies in biophysics and biochemistry which currently use synchrotron or x-ray laser sources [5] would benefit substantially from simpler intense sources in the so-called water window (2.3–4.4 nm). In this context, there is intensified interest in “direct,” efficient, x-ray production from laser-produced plasmas, using ultraintense ultrafast optical pulses [6].

Intense, short-duration keV x-ray pulse production in this case depends initially on the optical physics of interaction of intense light with near-solid plasma, and subsequently on the hydrodynamics of the plasma and the redistribution of absorbed energy within the material [7]. Specially nanostructured surfaces have been introduced, in an effort effectively to reduce the material surface-current response and the coherent scattering of laser light from flat solid surfaces. These surfaces greatly increase the optical absorptivity by depositing sootlike clusters of metal atoms (“smoke”), or by creating nanolithographic grating grooves in solid surfaces [8,9]; special prepulses have also been used to structure the plasma interaction surface so as to enhance surface-wave coupling, to similar effect [10]. Likewise, gas targets consisting of large clusters of noble-gas atoms have recently been investigated [11]. Since the efficiency of reradiation of laser energy as x rays

depends on the profiles of density and temperature within the plasma created, these target types have different conversion efficiencies and characteristic x-ray emission duration: short-duration pulses for nanogroove-grating targets, but at moderate conversion efficiency; higher conversion to x rays for smoke targets, but with pulse durations as long as a hundred picoseconds, and much longer for atomic clusters. Particularly, the initial density of material is a determining factor in the duration of the x-ray pulse, as may be the expansion divergence of the plasma created—initially spherical in the case of smoke clusters, and planar for nanolithographic groove targets.

Here we introduce a qualitatively new optically anisotropic material useful for targets, intermediate in type to smoke and nanogroove gratings, with a microscopic cylindrical geometry, and similarly large low-intensity absorption (~95%). This material consists of a surface of end-standing 10–200 nm diam metallic fibers, in a structure resembling velvet fabric, which may be cheaply fabricated from a range of different atomic elements from aluminum to platinum [12]. Individual fibers are near-solid density, and the overall density of the material is one-quarter to one-half solid. With an initial density similar to the nanogroove-grating target, and an expansion divergence intermediate to that of smoke and grating structures, these metallic velvets are found to produce high x-ray energy conversion (~0.01% for $h\nu > 900$ eV), similar to smoke targets, but with x-ray pulses of a few picosecond, similar to nanogroove-grating targets. In this combination, these “velvet” nanostructures produce the brightest x-ray pulses of the three types.

These velvet targets are electrochemically fabricated on Al substrates; their general characteristics and construction are described in detail elsewhere [12]. Three features of the process, attractive for plasma physics experiments, are (1) a wide variety of metals and/or semiconductors can be used; (2) more than one element can be deposited simultaneously; (3) surfaces of large size and arbitrary shape can be processed to produce the desired velvet target.

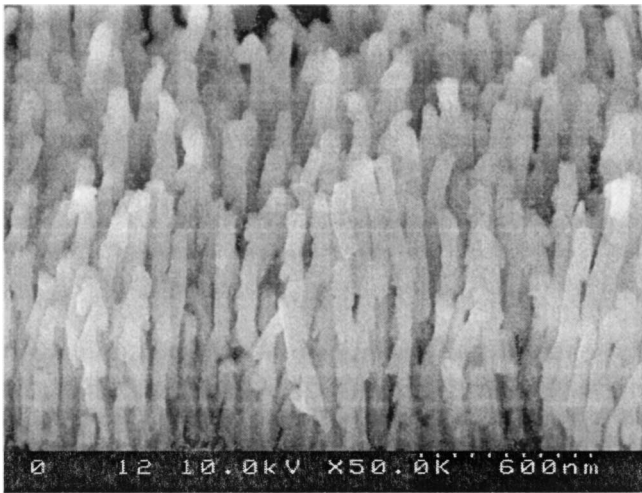


FIG. 1. Scanning electron micrograph of a Ni-nanowire target, showing a structure much like velvet fabric.

Figure 1 shows a scanning-electron microscope image of the surface of a Ni-velvet target used in this study. Wire diameters were 70 ± 5 nm and the wire spacing 100 ± 20 nm. Nanowire length was between 800 nm and $1 \mu\text{m}$. The target appearance in visible light is matte black.

The optical and laser-plasma characteristics of these targets were directly compared to Ni-black smoke targets, and Ni-coated Si nanogroove targets. The smoke targets were produced by evaporating nickel in an inert gas background of 2–10 Torr argon [13], depositing the sootlike condensate as a continuous layer on glass or metallic substrates in 20–30 μm layer thicknesses. The density was estimated to be 10^{-2} – 10^{-3} of solid density. The Ni-nanogroove targets were created by vacuum evaporating a 400–500-nm-thick Ni layer onto a lithographically produced silicon grating [14]. The spatial period of the rectangular-cross-section grating was $1.5 \mu\text{m}$, and the ridges were approximately $0.5 \mu\text{m}$ wide (fill fraction of 0.33).

The Toronto FCM-CPA Nd:glass terawatt laser system [15] was used for these experiments. It provided 1-ps pulses at $\lambda = 1.054 \mu\text{m}$, which were focused to a target spot size of $12 \mu\text{m}$ FWHM. Final pulse contrast, using a saturable-absorber cell, was at least 10^{10} . The angle of incidence for all experiments was 10° – 20° from the target normal.

A special filtered *p-i-n* photodiode (AXUV-100, International Radiation Detectors) was used to measure the integrated XUV emission in a narrow spectral range: the diode surface was coated with titanium/yttrium/carbon (6/210/55 nm), and the detector used in combination with a grazing-incidence gold mirror to create a bandpass filter centered at 125 eV with a FWHM of ± 90 eV. Two x-ray *p-i-n* photodiodes (UDT XUV-100) measured the integrated x-ray emission transmitted through a $12 \mu\text{m}$ Be filter (≥ 900 eV) for a $15 \mu\text{m}$ Al filter (≥ 1.5 keV). All detectors were used in photovoltaic mode with a low-input-impedance integrator circuit [16], providing a low-noise

linear response spanning 7 orders of magnitude of input energy. Detectors were placed $\sim 30^\circ$ from the surface normal, 0.5 m from the target. A collimator and magnetic baffle in front of each diode deflected energetic electrons.

Figure 2 summarizes the time-integrated x-ray yields from flat, nanogroove-grating, smoke and velvet targets, for *p*-polarized $1 \mu\text{m}$ pulses, as a function of incident laser energy. Absolute x-ray yield was obtained from the total integrated detector charge, using the manufacturer's specification for the typical quantum efficiency of the diode type and assuming uniform emission into 2π steradians.

In Fig. 2(a), the yield of XUV photons around 125 eV is plotted. In this soft range, nanowire and nanogroove-grating targets each produced yields about $4\times$ greater than that from the flat surface; the Ni-smoke surface shows a yield $14\times$ greater. Figure 2(b) shows that for x-ray energies above ~ 900 eV, the smoke and velvet surfaces show a yield increase of $50\times$ over the flat target, while the grating yield is only $10\times$ larger. Over the laser-energy

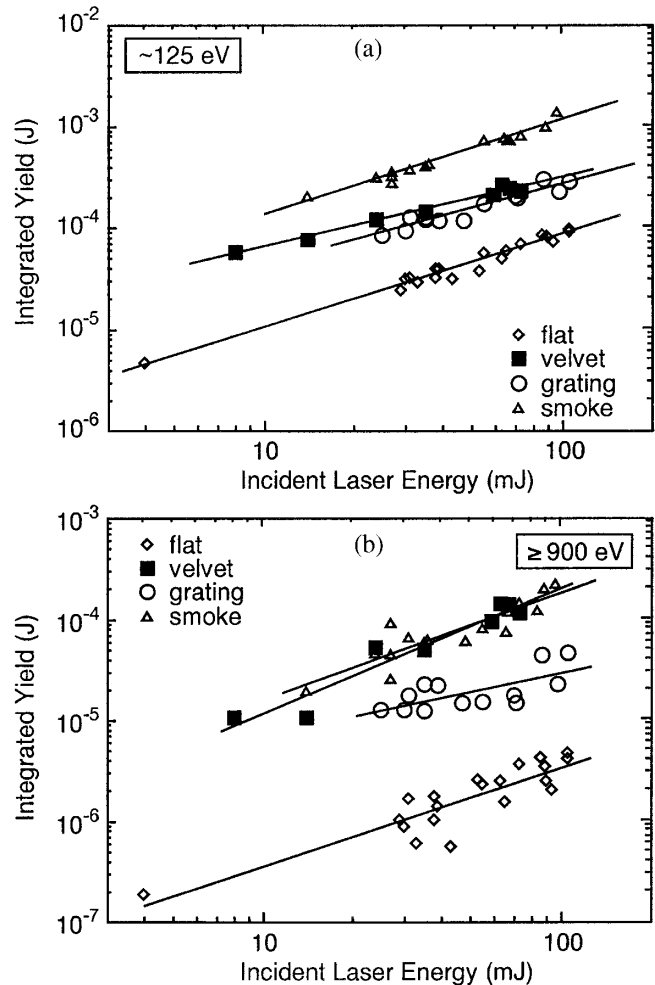


FIG. 2. Integrated absolute yield as a function of incident laser energy for each target type and energy range: (a) (125 \pm 90) eV, (b) >900 eV.

range studied, every yield has a power-law dependence on laser energy (E^α with $\alpha = 0.6-1.8$), and shows no saturation. Polarization was important only for the nanogroove structure—with s polarization the yield was dramatically reduced, as expected from previous absorption measurements [7].

A Kentech™ streak camera was used to measure the duration of the x-ray emission. Two different photocathodes were used: for XUV and soft-x-ray energies (>150 eV), a CsI photocathode (1359 Å) coated on 339-Å Al covering a 1- μm Lexan™ substrates; for x rays above ~ 1 keV, a photocathode consistent of a 330-Å layer of Au coated on a 12- μm layer of Be behind an additional 12- μm Be filter. The resolution of the streak camera is limited by the slit size and sweep speed to 8 ± 1 ps.

Time-dependent XUV and x-ray emission is shown in lineouts of the streaked images for the various target types (Fig. 3). As expected, the shortest x-ray pulses—nearly instrument limited at ~ 10 ps—were emitted from the near solid-density plasma of the flat target. Velvet nanowire and nanogroove-grating surfaces produced pulses of about 25 ps. The observed pulse length of approximately 70 ps from the Ni-smoke target is $8\times$ that of the pulse length emitted from the flat target.

The duration of keV x ray emission was found to be instrument-limited to less than 6 ps, after deconvolution, except for the Ni-smoke target, where there appears a weak slowly decaying tail. The high contrast of the laser pulse was found to be extremely important in keeping the high-energy x-ray emission short—the duration of the x-ray pulse tripled, while the yield advantage of the structured targets over the flat target disappeared, if the final pulse-cleaning dye cell was removed from the beam line.

We attribute the x-ray yield increase from the structured targets to at least three factors. First, structuring the target surface significantly enhances the small-signal absorption for the velvet nanowire, smoke, and nanogroove-grating

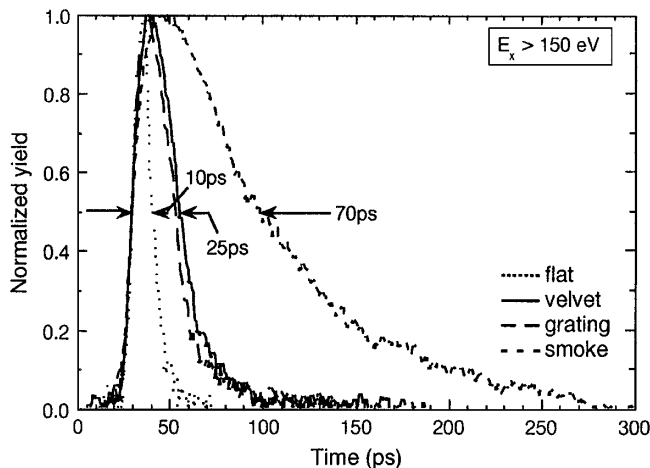


FIG. 3. Streak camera lineouts showing the duration of emission of XUV and soft-x-ray emission from velvet, smoke, grating, and flat Ni targets. Peaks are normalized for comparison.

targets—each appears nearly black in visible light. In the case of the velvet targets, the diameter of the nanowires is on the order of the skin depth—much less than the laser wavelength. Consequently, it is possible to describe the material by an effective dielectric, which will be anisotropic. Because of this anisotropy, Fresnel reflection at the interface is much reduced [16], therefore more light couples into the bulk of the material where it is strongly absorbed. Heuristically, the oriented nickel fibers principally support laser-driven currents along the target normal, for which the reradiation direction is parallel to the target surface; the target does not much support the components of current needed for specular Fresnel reflection.

Second, even after plasma formation the critical density surface of the target will be deeply convoluted, being positioned at the cylindrically expanding plasma around the nanowires, thus maintaining a large absorption coefficient in the high-intensity regime—an effect greatly exaggerating that of absorption increase by critical-surface rippling [17]. An upper limit Δr on the extent of radial plasma expansion from each of the heated Ni nanowires during irradiation can be estimated from the ion acoustic velocity, c_s , according to $\Delta r = \Delta \tau c_s = \Delta \tau (ZT_e/M)^{1/2}$. If the peak electron temperature is in the range 100–1000 eV, the resulting expansion in 1 ps is between 50–150 nm. Therefore, absent prepulses, closure of the voids in the structure is not expected until after most of the energy of the infrared pulse has been coupled-in, and high absorption is preserved in the laser-plasma interaction regime.

Third, although in the velvet target the density of the individual nanowires is initially near solid, and the average density of the material about one third of solid, both effective-dielectric modeling and our measurements of x-ray yield as a function of velvet-layer thickness show that the absorption depth is disproportionately large—on the order of 1 μm . Putting this in perspective: though the optical coupling depth (skin depth) for solid nickel at $\lambda = 1 \mu\text{m}$ is about 6 nm, during a 1 ps laser pulse at this intensity the laser will heat or ablate about a 100 nm depth of solid material to the point of producing soft x rays. Therefore, in the velvet target a depth of many more nickel atoms are heated, and so the temperature scale-length is also longer—both in laboratory coordinates and as indexed by areal density of material (i.e., both Eulerian and Lagrangian terms).

This leads to a situation a little like “exploding pusher” targets in laser fusion, in which a volume deposition of energy occurs, producing a more uniform plasma layer. It may also be that with a deeper layer the net opacity of the heated layer is larger, (i.e., smaller radiation escape factor) which may lead to higher temperatures, and greater conversion efficiency, as well as more nearly blackbody radiation. The observed dependence of keV x-ray yield on laser energy may bear this out: for the Stefan-Boltzmann radiation power relation $\sigma_B T^4$, and assuming the empirical approximation that electron temperature scales roughly

as $I^{1/3}$ [18], one expects roughly an $I^{1.3}$ scaling for black-body yield. The measured scaling for nanowire targets of $I^{(1.25 \pm 0.2)}$ is in good agreement.

The duration of emission by plasmas from each target type, and for each photon energy range, is principally determined by the falling edge of the x-ray pulse. This depends critically on the kinetic transport of the absorbed energy into the target, on plasma expansion, and on the efficiency of the radiative and nonradiative cooling processes. Heat flow in proportion to the temperature gradient of the plasma [19], but including a phenomenological flux limit [20], suggests the highest conductive cooling rates would be for the flat solid targets and the solid nanogroove-grating targets, since they presumably have the steepest temperature gradients. Velvet and smoke targets have larger absorption depths, due to their structure, and presumably smaller gradients of density and temperature. As well, expansional cooling might be expected to be slower for these plasmas, especially from the smoke targets, because macroscopically their large initial volumes require more time to double; however, microscopically this situation can be reversed, as the structured targets have larger initial divergence. Thus fast initial expansion may lead to collisional decoupling in the smoke targets while the plasma is still hot, and from this the two time scales observed for soft x-ray emission. Radiative cooling therefore becomes a more important cooling factor. Significantly, although smoke and nanowire targets may absorb 4 or 5 times as much energy as the flat solid targets, in keV x rays they radiate 40 or 50 times more. This disproportionality likely results from a combination of a larger number of heated atoms and the steep dependence of radiated power on temperature.

The smoke and velvet targets are distinguished by their geometries, but more importantly by their average densities, which differ by about 4 orders of magnitude. The low-density smoke targets will have reduced recombination rates, and be more prone to produce persistent resonance-line emission as the decoupling plasma approaches charge-state freezing. Velvet target plasmas are nearly solid average density, greatly increasing radiative recombination rates (and possibly also nonradiative three-body recombination rates). The major advantage of the velvet target is then that the nanowire fill-fraction can be altered to optimize absorption in the structure, but near-solid densities help to generate fast high intensity x-ray pulses from the laser plasma interaction.

In conclusion, we have made the first characterization of velvet nanostructured surfaces as highly efficient laser-plasma x-ray radiators, and compared them head-to-head with other nanostructured target surfaces and conventional solid targets. For keV x-rays, Ni velvet has about $50\times$ the efficiency of flat solid targets, and nearly the same emission duration. This material is inexpensive, scalable to large target surfaces and also to closed geometries; it is also physically much more robust than Ni smoke.

The authors would like to thank Professor Roger Falcone for generously providing nanogroove-grating substrates for the above experiments. We would also like to acknowledge useful discussions with Bin Xiao and Dr. Marc Le Flohic. This work was supported by the Natural Sciences and Engineering Research Council of Canada and by Photonics Research Ontario.

-
- [1] Ch. Spielmann *et al.*, *Science* **278**, 661 (1997); Z. Chang *et al.*, *Phys. Rev. Lett.* **79**, 2967 (1997).
 - [2] P. Gibbon, *Phys. Rev. Lett.* **76**, 50 (1996); P.A. Norreys *et al.*, *Phys. Rev. Lett.* **76**, 1832 (1996).
 - [3] J. Workman *et al.*, *Appl. Phys. Lett.* **70**, 312 (1997).
 - [4] M.H. Sher *et al.*, *Opt. Lett.* **12**, 891 (1987); H. Yamakoshi *et al.*, *J. Opt. Soc. Am. B* **13**, 436 (1996).
 - [5] D. Attwood *et al.*, *Science* **228**, 1265 (1985); B.J. McGowan *et al.*, *Phys. Rev. Lett.* **65**, 420 (1990).
 - [6] J.F. Pelletier *et al.*, *Appl. Phys. Lett.* **69**, 2172 (1996).
 - [7] H.M. Milchberg *et al.*, *Phys. Rev. Lett.* **61**, 2364 (1988); D.F. Price *et al.*, *Phys. Rev. Lett.* **75**, 252 (1995).
 - [8] M.M. Murnane *et al.*, *Appl. Phys. Lett.* **62**, 1068 (1993).
 - [9] S.P. Gordon *et al.*, *Opt. Lett.* **19**, 484 (1994).
 - [10] J.-C. Gauthier *et al.*, in *Applications of Laser Plasma Radiation II*, edited by M.C. Richardson and G.A. Kyrala, SPIE Proceedings Vol. 2523 (SPIE—International Society for Optical Engineering, Bellingham, WA, 1995), p. 306.
 - [11] T. Ditmire *et al.*, *Phys. Rev. Lett.* **75**, 3122 (1995).
 - [12] D. Al-Mawlawi, C.Z. Liu, and M. Moskovits, *J. Mater. Res.* **9**, 1014 (1994).
 - [13] L. Harris *et al.*, *J. Opt. Soc. Am. B* **42**, 134 (1952).
 - [14] Courtesy R. W. Falcone, Department of Physics, University of California at Berkeley, Berkeley, California.
 - [15] R.S. Marjoribanks *et al.*, *Opt. Lett.* **18**, 361 (1993).
 - [16] G. Kulcsár, Ph.D. dissertation, University of Toronto, 1998.
 - [17] R. A. Cairns, *Plasma Phys.* **20**, 991 (1978).
 - [18] Z. Jiang *et al.*, *Phys. Plasmas* **2**, 1702 (1995).
 - [19] L. Spitzer and R. Härm, *Phys. Rev.* **89**, 977 (1953).
 - [20] J. Delettrez, *Can. J. Phys.* **64**, 932 (1986).